Journal of Computational and Applied Mathematics 484 (2026) 117464

Contents lists available at ScienceDirect

Journal of Computational and Applied Mathematics

journal homepage: www.elsevier.com/locate/cam

A transported PDF modeling method applied to one-dimensional stochastic Burgers equation ⋆

Yize Wang [a,b], Li Yuan [a,b,*]

[a] ICMSEC & State Key Laboratory of Mathematical Sciences, Academy of Mathematics and Systems Science, Chinese Academy of Sciences, Beijing 100190, PR China
[b] School of Mathematical Sciences, University of Chinese Academy of Sciences, Beijing 100049, PR China

ARTICLE INFO

Keywords:
Burgers turbulence
Probability density function
Closure
Monte carlo method
Quadrature based moment method
Moment inversion

ABSTRACT

In this paper we apply the transported probability density function (PDF) method to model the Burgers turbulence governed by the one-dimensional Burgers equation with a stochastic external force and random initial data. The PDF modeling method can provide the mean and high order moments of the random solution variable which are useful for the characterization of Burgers turbulence. Firstly, an exact one-point PDF transport equation is derived from the Burgers equation with a stochastic external force, and then the conditional advection and diffusion terms are modeled for closure by using two respective models. Secondly, three numerical methods are employed to solve the modeled PDF transport equation: the mesh-based Lagrangian particle Monte Carlo (MC) method, the original quadrature method of moments (QMOM), and the linear QMOM (LQMOM) as modified in this work. The numerical tests verify the viability of using the PDF modeling method to study Burgers turbulence and show that the MC method, LQMOM and QMOM can yield results comparable to the DNS solution, and the LQMOM is more efficient than the QMOM and MC method. However, the MC method has less dissipation for turbulence in high wavenumber regimes.

1. Introduction

The nonlinear and the Laplacian terms in the one-dimensional (1D) Burgers equation can be seen to mimic the convective and dissipative mechanisms of real fluid flows. Therefore the Burgers equation is extensively used as a prototype model to investigate different characteristics of turbulence [1–8], to test different averaging and closure models for turbulent flows [9–16] and to validate different novel computational schemes [17–19].

The Burgers turbulence resulting from the solution of the 1D Burgers equation with stochastic forcing terms and/or random initial conditions exhibits random fluctuations in space and time. The statistical properties of Burgers turbulence depend strongly on the probability distributions of both the initial data and the additive random forcing term [13]. Under specific conditions Burgers turbulence may mimic some characteristics of compressible turbulent flows like shocks, intermittency and energy cascades. Similar to cases with real turbulent flows, large-eddy simulation (LES) [9–12,14,15] and direct numerical simulation (DNS) [14,20] methods have been employed to study Burgers turbulence. The transported probability density function (PDF) method belongs to another type

⋆ This work is funded by National Key R&D Plan of China (Grant No. 2024YFA1012500) and National Natural Science Foundation of China (Grant Nos. 12071470, 12161141017, 12494543).

* Corresponding author.
E-mail addresses: wangyize@lsec.cc.ac.cn (Y. Wang), lyuan@lsec.cc.ac.cn (L. Yuan).

https://doi.org/10.1016/j.cam.2026.117464
Received 18 May 2025; Received in revised form 18 January 2026
Available online 20 February 2026
0377-0427/© 2026 Elsevier B.V. All rights are reserved, including those for text and data mining, AI training, and similar technologies.

of turbulence modeling method and it has long been applied to model turbulent non-reacting [21–23] and reacting flows [24–27]. The main advantage of the PDF method is that it enables exact closure of the nonlinear chemical source terms with Reynolds averaging or LES filtering. Thus applying the PDF method to model Burgers turbulence is also suitable, particularly when the stochastic forcing term in the Burgers equation is a nonlinear function of the solution variable. In the PDF method, the one-point PDF of the solution variable (velocity) can provide the mean velocity and any order statistical moments of importance such as the turbulent kinetic energy.

In the past decades the Monte Carlo (MC) method [28] has been applied to evaluate the path integral formulation for the stochastic Burgers equation [18]. The MC method has also been used to sample a sufficiently large number of solutions to the stochastic Burgers equation and the averaged results are compared with the discontinuous Galerkin solution to the reduced one-point and two-point PDF equations of the solution field [13]. However, the conditional diffusion term even in the reduced one-point PDF equation in [13] was computed by a separate MC method and thus the PDF equation is not autonomous. To the best knowledge of the present authors, there is no closed one-point PDF transport equation for Burgers turbulence in the literature. The closure of the one-point PDF equation will be the first focus of this work.

The second focus of this work is on developing an efficient solution method for the closed PDF transport equation. Generally, a PDF transport equation is high-dimensional in the sense that it has multiple internal coordinates, and thus traditional numerical methods like finite difference and finite volume methods are not suitable. In convention, Lagrangian MC methods employing an ensemble of notional particles are widely used for numerically solving the PDF transport equation for turbulent reactive flows [29,30]. The computational cost of Lagrangian MC methods increases linearly with the dimension of the PDF. However, the statistic error of Lagrangian MC methods is inversely proportional to the square root of the number of notional particles. To reduce the statistic error, more particles need to be used which may incur an increase in computational cost. Alternatively, Eulerian stochastic field (ESF) methods using the average of sample solutions to the stochastic partial differential equations that are equivalent to the original PDF equation for turbulent combustion are also used [25,31,32]. However, ESF methods need special attention to the discretization of spatial terms. The efficiency and accuracy are generally inferior to Lagrangian MC methods.

In recent years, deterministic solution methods for PDF equations such as the quadrature based moment method (QBMM) have emerged. In general, QBMMs solve the spatio-temporal moment transport equations corresponding to the original PDF transport equation and thus traditional methods like finite difference method are applicable. The main idea of QBMM is to use the transported moments to reconstruct an approximate PDF distribution (called moment inversion process), and the reconstructed information can be used to compute the unclosed chemical reaction source terms and other nonlinear source terms appearing in the moment transport equations. After the original quadrature method of moments (QMOM) was first introduced by Mcgraw [33] for describing the aerosol dynamics, different variants of QBMMs were developed and applied to various kinds of PDF equations like population balance equations in dispersive multi-phase flows [34,35], gas kinetic equations [36,37] and the PDF transport equation for turbulent combustion [38–41]. So it is meaningful to study the pros and cons of QBMMs and MC methods in the relatively simple 1D Burgers turbulence problem before these methods can be applied in more practical applications.

In this work, we develop a closed-form PDF transport equation for modeling the 1D Burgers turbulence and improve a numerical method for solving this equation. Firstly, an exact one-point PDF transport equation with velocity as the internal coordinate is derived from the 1D Burgers equation with a stochastic forcing term, and the conditional advection and diffusion terms, which require multi-point information, are modeled for closure by using a lumped gradient model proposed in this work and the Interaction by Exchange with the Mean (IEM) micromixing model from the literature [42–44], respectively. Secondly, we make a modification to the linear-inversion-based quadrature method of moments (LQMOM) proposed in [45] to ensure the positivity of the reconstructed PDF values. Thirdly, we apply three methods, i.e., the MC method [46], the original QMOM [33] and the presently modified LQMOM to solve the modeled PDF transport equation and compare the numerical results and computational costs with DNS of the Burgers equation. The numerical results confirm the effectiveness of the modeled PDF transport equation and the modified LQMOM.

The rest of the paper is organised as follows. In Section 2, we give the derivation of the PDF transport equation, the closure models, the modeled PDF equation, and the corresponding moment transport equations. In Section 3, we give a brief introduction to the MC method and QMOM and a detailed description of the presently modified LQMOM. In Section 4, we provide three numerical Burgers equation examples with random initial conditions or random external forcing terms. Section 5 gives our concluding remarks.

2. Transported PDF model for Burgers turbulence

In this section, the derivation of an exact PDF transport equation and the closure of this equation are given.

2.1. Derivation of PDF equation

In this subsection, we derive an exact one-point velocity PDF transport equation for describing Burgers turbulence through the use of fine-grained PDF. Let us consider the following canonical initial-boundary value problem for the Burgers equation with a random external forcing term, a random initial condition and periodic boundary conditions,

$$\begin{cases} \dfrac{\partial u}{\partial t} + u\dfrac{\partial u}{\partial x} = \nu\dfrac{\partial^2 u}{\partial x^2} + S(u,x,t), \quad -1 < x < 1,\ t > 0, \\ u(x,0) = u_0(x), \\ u(-1,t) = u(1,t), \end{cases} \tag{1}$$

where the initial condition $u_0(x)$ and the forcing term $S(u,x,t)$ are random fields with a given distribution in the respective sample space. Notice that $S(u,x,t)$ may nonlinearly depends on u in addition to x and t.

The fine-grained PDF is defined for the stochastic solution variable $u(x,t)$ which represents the velocity at a point x and a time t, and is given by

$$f^*(v,u(x,t)) = \delta(v-u(x,t)), \tag{2}$$

where v denotes the sample space of $u(x,t)$.

The fine-grained PDF (2) has the following property:

$$\langle f^*(v,u(x,t))\rangle = \int_{-\infty}^{\infty} \delta(v-v')f(v';x,t)\,\mathrm{d}v' = f(v;x,t), \tag{3}$$

where $\langle\cdot\rangle$ denotes the probabilistic average over the sample space of $u(x,t)$, and $f(v;x,t)$ is the probability density function of the random variable $u(x,t)$. The semicolon is used to separate the sample space variable v from the location and time variables.

For any random variable Q (or random variable function $R(u)$), there is the following important conclusion which is frequently used in the derivation of the PDF equation:

$$\langle Q f^*(v,u(x,t))\rangle = \langle Q|u=v\rangle f(v;x,t), \quad \text{and the corollary: } \langle R(u)f^*(v,u(x,t)) = R(v)f(v;x,t). \tag{4}$$

Now we proceed to derive a one-point PDF transport equation for the Burgers equation (1). The method of derivation involves directly calculating the probabilistic average of the material derivative $Df^*/Dt := f^*_t + uf^*_x$ following the method outlined in [44]. First, we take the derivatives of f^* with regard to t and x,

$$\frac{\partial f^*}{\partial t} = \frac{\partial f^*}{\partial u}\frac{\partial u}{\partial t} = -\frac{\partial f^*}{\partial v}\frac{\partial u}{\partial t}, \tag{5}$$

$$\frac{\partial f^*}{\partial x} = \frac{\partial f^*}{\partial u}\frac{\partial u}{\partial x} = -\frac{\partial f^*}{\partial v}\frac{\partial u}{\partial x}. \tag{6}$$

By manipulating (5) + $u\times$(6) and using the Burgers equation (1), we have

$$\frac{\partial f^*}{\partial t} + u\frac{\partial f^*}{\partial x} = -\frac{\partial f^*}{\partial v}\left(\frac{\partial u}{\partial t} + u\frac{\partial u}{\partial x}\right) \overset{(1)}{=} -\frac{\partial f^*}{\partial v}\left(\nu\frac{\partial^2 u}{\partial x^2} + S(u,x,t)\right) = -\frac{\partial}{\partial v}\left(f^*\nu\frac{\partial^2 u}{\partial x^2} + f^*S(u,x,t)\right). \tag{7}$$

Next, we take the probabilistic average of Eq. (7). Using the interchangeability between the expectation and the derivatives with regard to t and the property (3), we get

$$\frac{\partial f}{\partial t} + \left\langle u\frac{\partial f^*}{\partial x}\right\rangle = \left\langle -\frac{\partial}{\partial v}\left(f^*\nu\frac{\partial^2 u}{\partial x^2} + f^*S(u,x,t)\right)\right\rangle. \tag{8}$$

For the second term on the left-hand side (LHS) of Eq. (8) with $\partial f^*/\partial x$, we first rewrite it as a conservative term and a term without $\partial f^*/\partial x$ and then apply the conclusion (4) to achieve

$$\left\langle u\frac{\partial f^*}{\partial x}\right\rangle = \left\langle\frac{\partial(uf^*)}{\partial x}\right\rangle - \left\langle\frac{\partial u}{\partial x}f^*\right\rangle \overset{(4)}{=} \frac{\partial(vf)}{\partial x} - \left\langle\frac{\partial u}{\partial x}\middle| u=v\right\rangle f. \tag{9}$$

Notice that the last term on the right-hand side (RHS) of Eq. (9) is an additional term due to the unavailability of the continuity equation, which vanishes for the case with real fluid flow. This term poses difficulty for the closure and requires special attention in the subsequent modeling.

Using Leibniz integral rule and the properties (3) and (4), the RHS of Eq. (8) becomes

$$\left\langle -\frac{\partial}{\partial v}\left(f^*\nu\frac{\partial^2 u}{\partial x^2} + f^*S(u,x,t)\right)\right\rangle = -\frac{\partial}{\partial v}\left(\left\langle\nu\frac{\partial^2 u}{\partial x^2}\middle| u=v\right\rangle f + S(v,x,t)f\right). \tag{10}$$

Alternatively, by making use of the following result (Exercise 12.54 in Pope's book [44])

$$\nabla^2 f^* = -\frac{\partial}{\partial v}\left(f^*\nabla^2 u\right) + \frac{\partial^2}{\partial v^2}\left(f^*\nabla u\cdot\nabla u\right)$$

and multiplying both sides of it with the constant ν, and then taking the expectation, we can obtain

$$-\frac{\partial}{\partial v}\left(\left\langle\nu\frac{\partial^2 u}{\partial x^2}\middle| u=v\right\rangle f\right) = \nu\frac{\partial^2 f}{\partial x^2} - \frac{\partial^2}{\partial v^2}\left(\left\langle\nu\frac{\partial u}{\partial x}\frac{\partial u}{\partial x}\middle| u=v\right\rangle f\right). \tag{11}$$

Here, the first term in the RHS is the diffusion in the physical space and the second term is the mixing in the velocity space due to the conditional dissipation. Substituting Eqs. (9) and (10) with (11) into Eq. (8), we arrive at the exact PDF transport equation

$$\frac{\partial f}{\partial t} + \frac{\partial(vf)}{\partial x} - \left\langle\frac{\partial u}{\partial x}\middle| u=v\right\rangle f = \nu\frac{\partial^2 f}{\partial x^2} - \frac{\partial^2}{\partial v^2}\left(\left\langle\nu\frac{\partial u}{\partial x}\frac{\partial u}{\partial x}\middle| u=v\right\rangle f\right) - \frac{\partial}{\partial v}\left(S(v,x,t)f\right). \tag{12}$$

Eq. (12) is a high-dimensional transport equation with respect to t, x, and v. The two conditional expectation terms involve multi-point information, thus requiring closure. The LHS conditional term is new while the RHS conditional term is similar to a part of the conditional diffusion term in the scalar joint PDF transport equation for turbulent combustion [24,27,44]. The nonlinear term is closed since S depends on v explicitly. However, because S contains some random parameter with a given distribution in the corresponding sample space, Eq. (12) is a stochastic partial differential equation.

For ease of closure, we decompose the velocity u into the probability-averaged mean $\langle u\rangle = \int_{-\infty}^{\infty} v f(v)\,\mathrm{d}v$ and the fluctuating part u', $u = \langle u\rangle + u'$. In this way, Eq. (12) becomes

$$\frac{\partial f}{\partial t} + \frac{\partial (vf)}{\partial x} - \frac{\partial \langle u\rangle}{\partial x} f - \left\langle \frac{\partial u'}{\partial x}\middle| u = v \right\rangle f = \nu \frac{\partial^2 f}{\partial x^2} - \frac{\partial^2}{\partial v^2}\left(\left\langle \nu \frac{\partial u}{\partial x}\frac{\partial u}{\partial x}\middle| u = v \right\rangle f \right) - \frac{\partial}{\partial v}\big(S(v,x,t) f\big). \tag{13}$$

Before making closure for Eq. (13), let us consider what constraints the two conditional terms should satisfy. The constraint on conditional diffusion term in the RHS has been discussed in Fox's book [47], so we focus on the constraint on the conditional term in the LHS.

By multiplying Eq. (13) by v and integrating over the v space, we obtain the first-order moment equation:

$$\begin{aligned} &\frac{\partial \langle u\rangle}{\partial t} + \frac{1}{2}\frac{\partial \langle u^2\rangle}{\partial x} + \underline{\frac{1}{2}\frac{\partial \langle u^2\rangle}{\partial x} - \frac{1}{2}\frac{\partial \langle u\rangle^2}{\partial x} - \int_{-\infty}^{\infty} \left\langle \frac{\partial u'}{\partial x}\middle| u = v \right\rangle v f\,\mathrm{d}v} = \nu \frac{\partial^2 \langle u\rangle}{\partial x^2} \\ &- v\frac{\partial}{\partial v}\left(\left\langle \nu \frac{\partial u}{\partial x}\frac{\partial u}{\partial x}\middle| u = v \right\rangle f \right)\Big|_{v=-\infty}^{v=\infty} + \left\langle \nu \frac{\partial u}{\partial x}\frac{\partial u}{\partial x}\middle| u = v \right\rangle f\Big|_{v=-\infty}^{v=\infty} + \int_{-\infty}^{\infty} S(v,x,t) f\,\mathrm{d}v. \end{aligned} \tag{14}$$

If we use the argument that $f(v;x,t)$ is a "well behaved" PDF and the other terms are "well behaved" functions (see P.247 in [47]), the second and third terms on the RHS of Eq. (14) vanish. The remaining terms except the underlined terms represent the statistical average of the Burgers equation (1). To make Eq. (14) identical with the statistical average of Eq. (1), the underlined terms should vanish. Thus we have the constraint

$$-\int_{-\infty}^{\infty} \left\langle \frac{\partial u'}{\partial x}\middle| u = v \right\rangle v f\,\mathrm{d}v = \frac{1}{2}\frac{\partial \langle u\rangle^2}{\partial x} - \frac{1}{2}\frac{\partial \langle u^2\rangle}{\partial x}, \tag{15}$$

which states that the integral term in Eq. (15) is equal to the gradient of the Reynolds stress, $(\tau_{\mathrm{sgs}})_x$, of the statistically averaged Burgers equation, $\langle u\rangle_t + \frac{1}{2}\big(\langle u\rangle^2\big)_x = \nu\langle u\rangle_{xx} + (\tau_{\mathrm{sgs}})_x + \langle S\rangle$, where $\tau_{\mathrm{sgs}} = \frac{1}{2}\big(\langle u\rangle^2 - \langle u^2\rangle\big)$.

2.2. Closure of the PDF equation

Following the literature [24–27,47], the second term on the RHS of Eq. (13) can be modeled using the IEM (the interaction by exchange with the mean) micromixing model [42,43],

$$-\frac{\partial^2}{\partial v^2}\left(\left\langle \nu \frac{\partial u}{\partial x}\frac{\partial u}{\partial x}\middle| u = v \right\rangle f \right) \approx \frac{\partial}{\partial v}\big[\Omega_m (v - \langle u\rangle) f\big]. \tag{16}$$

Here, Ω_m is the mixing frequency to be given later.

For the fourth term on the LHS of Eq. (13), we see from Eq. (15) that its integral mimics the x-derivative of the Reynolds stress $0.5\big(\langle u\rangle^2 - \langle u^2\rangle\big)$. In analogy with the RANS/LES approach, we propose a naive gradient model:

$$-\left\langle \frac{\partial u'}{\partial x}\middle| u = v \right\rangle f \approx \frac{\partial}{\partial x}\left(\Gamma_{t1}\frac{\partial f}{\partial x} \right), \tag{17}$$

where $\Gamma_{t1} \geq 0$ is an eddy viscosity that depends on $\langle u\rangle$ and thus on f. Notice that this term plays a role of negative diffusion in Eq. (13). We will modify this naive gradient model after introducing Eq. (18).

Thus, with the models (16) and (17), the PDF equation (13) can be closed as follows:

$$\frac{\partial f}{\partial t} + \frac{\partial (vf)}{\partial x} - \frac{\partial \langle u\rangle}{\partial x} f + \frac{\partial}{\partial x}\left(\Gamma_{t1}\frac{\partial f}{\partial x} \right) = \nu \frac{\partial^2 f}{\partial x^2} + \frac{\partial}{\partial v}\big[\Omega_m (v - \langle u\rangle) f\big] - \frac{\partial}{\partial v}\big(S(v,x,t) f\big). \tag{18}$$

However, our experience indicates that numerical solution of Eq. (18) always diverges even if we artificially set $\Gamma_{t1} < 0$ to get a positive diffusion term. To overcome this issue, we modify Eq. (18) as follows. We split the advection term as $\frac{\partial (vf)}{\partial x} = \frac{\partial \langle u\rangle f}{\partial x} + \frac{\partial (v - \langle u\rangle) f}{\partial x}$, and intentionally model the second term (which looks like the residual part in LES) by using an approximate gradient model as $\frac{\partial (v - \langle u\rangle) f}{\partial x} \approx -\frac{\partial}{\partial x}\left(\Gamma_{t2}\frac{\partial f}{\partial x} \right)$, $\Gamma_{t2} \geq 0$. Then we combine it with the model (17) to obtain a lumped gradient model:

$$\frac{\partial (v - \langle u\rangle) f}{\partial x} - \left\langle \frac{\partial u'}{\partial x}\middle| u = v \right\rangle f \approx -\frac{\partial}{\partial x}\left[\big(\Gamma_{t2} - \Gamma_{t1}\big)\frac{\partial f}{\partial x} \right] = -\frac{\partial}{\partial x}\left(\Gamma_t \frac{\partial f}{\partial x} \right), \tag{19}$$

where $\Gamma_t = \Gamma_{t2} - \Gamma_{t1}$ is a lumped turbulent diffusion coefficient which must be constrained to be positive. Note that Γ_{t1} and Γ_{t2} are no longer required; instead, only Γ_t matters. By using the split advection terms and the lumped gradient model (19) in Eq. (18), we obtain the final modeled PDF transport equation adopted in this work:

$$\frac{\partial f}{\partial t} + \langle u\rangle \frac{\partial f}{\partial x} = \frac{\partial}{\partial x}\left(\big(\nu + \Gamma_t\big)\frac{\partial f}{\partial x} \right) + \frac{\partial}{\partial v}\big[\Omega_m (v - \langle u\rangle) f\big] - \frac{\partial}{\partial v}\big(S(v,x,t) f\big). \tag{20}$$

The moment transport equations can be derived by multiplying Eq. (20) by v^n and integration, which yields:

$$\frac{\partial M_k}{\partial t} + M_1 \frac{\partial M_k}{\partial x} = \frac{\partial}{\partial x}\left(\big(\nu + \Gamma_t\big)\frac{\partial M_k}{\partial x} \right) + k\Omega_m (M_1 M_{k-1} - M_k) + k\int_{-\infty}^{\infty} S(v,x,t) v^{k-1} f\,\mathrm{d}v, k = 0, 1, \cdots, \tag{21}$$

where the k-th order moment $M_k = \int_{-\infty}^{\infty} v^k f(v)\,\mathrm{d}v$. Notice that if the forcing term has the form $S(v,x,t) = S(x,t)$, the last term on the RHS of Eq. (21) reduces to $kM_{k-1}S(x,t)$, thus Eq. (21) is closed and can be solved using the classical moment method, and thus QBMMs are unnecessary.

Compared with Eq. (18), the Eq. (20) has two advantages: 1) the corresponding moment equations do not contain a higher order moment in the advection terms which usually needs an extra closure; 2) it has better numerical stability as experienced.

The mixing frequency Ω_m and turbulent viscosity Γ_t can be calculated from the Smagorinsky model as follows:

$$\Omega_m = C_\Omega \frac{\nu + \Gamma_t}{\Delta^2}, \quad \Gamma_t = (C_S \Delta)^2 \left| \frac{\partial \tilde{u}}{\partial x} \right|. \tag{22}$$

In this work, we take the viscosity constant $\nu = 8 \times 10^{-5}$ as in [14], the free parameter $C_\Omega = 4$, the Smagorinsky constant $C_S = 0.17$, and the filtering width Δ to be the grid size in the mesh-based Lagrangian MC method [29] and QBMMs. The filtered velocity $\tilde{u}$ in Eq. (22) is taken to be the ensemble-averaged solution $\langle u \rangle$ in the MC method or the first-order moment M_1 in QBMMs.

3. Implementation of MC and QBMMs

In this section, we introduce the Monte Carlo method [29] and two QBMMs (QMOM [33] and LQMOM [45]).

3.1. MC method

The mesh-based Lagrangian Monte Carlo algorithm [29,44,46] is employed for the numerical solution of Eq. (20). Particles move in the physical space due to the particle velocity, which is governed by a simplified Langevin model (SLM) corresponding to the Burgers equation (1). This SLM is directly adapted from the same-named model for the incompressible Navier-Stokes equations [44,48]. The location $X^{(n)}(t)$ and velocity $u^{(n)}(t)$ of the n-th particle in the computational domain are evolved according to the following stochastic differential equations:

$$\mathrm{d}X^{(n)}(t) = u^{(n)}(t)\mathrm{d}t, \tag{23a}$$

$$\mathrm{d}u^{(n)}(t) = \left[S\left(u^{(n)}(t), X^{(n)}(t), t\right) + \nu \left(\nabla^2 \langle u \rangle\right)^* - \left(\frac{1}{2} + \frac{3}{4} C_0\right) \Omega_m^* \left(u^{(n)}(t) - \langle u \rangle^*\right) \right] \mathrm{d}t + \left(C_0 k^* \Omega_m^*\right)^{1/2} \mathrm{d}W(t), \tag{23b}$$

where the constant $C_0 = 2.1$ and $k = \frac{1}{2}\left(\langle u^2 \rangle - \langle u \rangle^2\right)$ is the turbulent kinetic energy. The superscript "$*$" on $\langle u \rangle$, $\nabla^2 \langle u \rangle$, k, and Ω_m denotes that the values are taken at the particle location $X^{(n)}(t)$ and interpolated from their respective particle-field values (ensemble averages) at grid points at the time t, which will be introduced later. $\mathrm{d}W(t)$ denotes the Wiener process associated with a particle, providing randomness to the velocity increment of the particle. The drift and diffusion coefficients are obtained by comparing the Fokker-Planck equation corresponding to Eq. (23b) with the PDF transport equation (23).

The Eqs. (24a) and (24b) are advanced in time by using a first-order explicit Euler scheme as follows:

$$X^{(n)}(t_{i+1}) = X^{(n)}(t_i) + u^{(n)}(t_i)\Delta t, \tag{24a}$$

$$u^{(n)}(t_{i+1}) = u^{(n)}(t_i) + \left[S\left(u^{(n)}(t_i), X^{(n)}(t_i), t_i\right) + \nu \left(\frac{\partial^2 \langle u \rangle}{\partial x^2} \right)^* - \left(\frac{1}{2} + \frac{3}{4} C_0\right) \Omega_m^* \left(u^{(n)}(t_i) - \langle u \rangle^*\right) \right] \Delta t + \left(C_0 k^* \Omega_m^* \Delta t\right)^{1/2} \xi_{i+1}^{(n)}, \tag{24b}$$

where i indicates the time level, $\Delta t = t_{i+1} - t_i$ is the time step, and $\xi_{i+1}^{(n)}$ are Gaussian pseudo-random numbers following the standard Gaussian distribution.

In order to obtain the interpolated quantities with "*" in Eq. (24b), the ensemble averages $\langle u \rangle$ and $\langle u^2 \rangle$ at grid points are required. Let N_E be the number of particles in a sampling volume $\Delta V_j = [x_{j-1}, x_{j+1}]$ centered at the grid point x_j. Particles within ΔV_j are collectively assigned to the grid point x_j. Assume that the grid is uniform with the grid size Δx. The ensemble averages at the grid point x_j are estimated by taking the average of the particles within ΔV_j using the "tent function" defined as follows [46]:

$$B_j(x) = \begin{cases} 1 - \dfrac{|x - x_j|}{\Delta x} & \text{if} \quad |x - x_j| < \Delta x, \\ 0 & \text{otherwise.} \end{cases} \tag{25}$$

$\langle u \rangle$ and $\langle u^2 \rangle$ on the grid are estimated by using the weighted average of particles within the sampling volume:

$$\langle u \rangle_j = \frac{\sum_{n \in \Delta V_j} B_j\left(X^{(n)}\right) u^{(n)}}{\sum_{n \in \Delta V_j} B_j\left(X^{(n)}\right)}, \quad \langle u^2 \rangle_j = \frac{\sum_{n \in \Delta V_j} B_j\left(X^{(n)}\right) \left(u^{(n)}\right)^2}{\sum_{n \in \Delta V_j} B_j\left(X^{(n)}\right)}, \tag{26}$$

and the turbulent kinetic energy on the grid is given by [27]

$$k_j = \frac{1}{2}\left(\langle u^2 \rangle_j - \langle u \rangle_j^2\right). \tag{27}$$

Once all $\langle u \rangle_j$ on the grid have been computed, we can compute $\nabla \langle u \rangle$ and $\nabla^2 \langle u \rangle$ at the grid point x_j by using the central difference scheme as follows:

$$\left(\frac{\partial \langle u \rangle}{\partial x} \right)_j = \frac{\langle u \rangle_{j+1} - \langle u \rangle_{j-1}}{2\Delta x}, \quad \left(\frac{\partial^2 \langle u \rangle}{\partial x^2} \right)_j = \frac{\langle u \rangle_{j-1} - 2\langle u \rangle_j + \langle u \rangle_{j+1}}{\Delta x^2}. \tag{28}$$

And the mixing frequency $(\Omega_m)_j$ can be calculated using Eq. (22) with $\tilde{u} = \langle u \rangle$, $\Delta = \Delta x$ and the first equality of Eq. (28).

Values of $\langle u \rangle^*, (\nabla^2 \langle u \rangle)^*, k^*$ and Ω_m^* at the particle location $X^{(n)}(t)$ as needed by Eq. (24b) are obtained by interpolating the corresponding values at grid points. In this work, the interpolations from grid points to the particle position is performed by using a five-point Lagrange interpolation method.

3.2. QMOM and LQMOM

In the original QMOM [33,47], the PDF is approximated by a weighted sum of Dirac delta functions:

$$f(v;x,t) \approx \sum_{j=1}^{N_q} w_j(x,t)\delta\big(v - v_j(x,t)\big), \tag{29}$$

where w_j is the weight, v_j is the abscissa, and N_q is the number of quadrature nodes in the sample space. Using Eq. (29), the source integral term in the moment transport equations (21) can be written as

$$\int_{-\infty}^{\infty} v^{k-1} S(v) f(v)\,\mathrm{d}v = \sum_{j=1}^{N_q} w_j v_j^{k-1} S\big(v_j\big). \tag{30}$$

Eq. (30) means that the closure of nonlinear source terms is transferred to the calculation of weights w_j and abscissas v_j. Eq. (29) also enables the moments to be expressed in terms of w_j and v_j:

$$M_k = \int_{-\infty}^{\infty} v^k f(v)\,\mathrm{d}v = \sum_{j=1}^{N_q} w_j v_j^k. \tag{31}$$

At every grid point and every time, a set of $2N_q$ nonlinear equations, Eq. (31), is solved for the unknowns w_j and $v_j, j = 1, \ldots, N_q$, given $2N_q$ integer moments $(M_0, M_1, \ldots, M_{2N_q-1})$ from the numerical solution of Eq. (21). The solution of Eq. (31) is called moment inversion. For the univariate PDF case, the product-difference (PD) [33,49] or the Wheeler algorithm [50,51] can be used to solve w_j and v_j efficiently. In this paper, we use the PD algorithm.

Very recently, we developed the linear quadrature method of moments (LQMOM) [45]. In this method, the shape of PDF is no longer presumed and the PDF and source function $S(v)$ are assumed to be smooth in v such that a conventional quadrature rule can be used to approximate the moments and source integral terms. For the 1D sample space $v \in \mathbb{R}$, we have

$$M_k = \int_{-\infty}^{\infty} v^k f(v)\,\mathrm{d}v \approx \sum_{j=1}^{N_L} \omega_j v_j^k f_j, \tag{32}$$

$$\int_{-\infty}^{\infty} v^{k-1} S(v) f(v)\,\mathrm{d}v \approx \sum_{j=1}^{N_L} \omega_j v_j^{k-1} S(v_j) f_j, \tag{33}$$

where v_j and ω_j are N_L predefined quadrature nodes and weights in the sample space, and $f_j = f(v_j)$ are the PDF values at the quadrature nodes. In the special case when $f(v)$ is a polynomial of degree $(N_L - 1)$, Eq. (32) is exact.

Take the number of quadrature nodes $N_L = 4$ as an example. We can write Eq. (32) as the linear system of equations:

$$\begin{bmatrix} \omega_1 & \omega_2 & \omega_3 & \omega_4 \\ \omega_1 v_1 & \omega_2 v_2 & \omega_3 v_3 & \omega_4 v_4 \\ \omega_1 v_1^2 & \omega_2 v_2^2 & \omega_3 v_3^2 & \omega_4 v_4^2 \\ \omega_1 v_1^3 & \omega_2 v_2^3 & \omega_3 v_3^3 & \omega_4 v_4^3 \end{bmatrix} \begin{bmatrix} f_1 \\ f_2 \\ f_3 \\ f_4 \end{bmatrix} = \begin{bmatrix} M_0 \\ M_1 \\ M_2 \\ M_3 \end{bmatrix}. \tag{34}$$

If the size of the linear system is N_L, we need to solve N_L moment transport equations in order to provide the N_L moments in Eq. (34) ($M_0 \equiv 1$ need not be solved). The computer time for solving this linear system of size N_L is much smaller than that for solving the same sized nonlinear system (31) as in the QMOM.

In this paper, we fix the bug with the LQMOM [45] which may generate negative PDF values in the solution of Eq. (34) when the underlying PDF distribution is sharp or discontinuous. This is done as follows. For the tentative solution $f_1, f_2, \ldots, f_{N_L}$, we check the sign of each element f_i and make a correction to the whole solution if $f_i < 0$, in the order of $i = 1, \ldots, N_L$. In this correction, we modify the current element f_i to zero and denote the new value as $F_i = 0$, and modify all the other elements f_k to new values F_k according to the formula

$$F_k = f_k \cdot \frac{M_0}{\sum_{j=1}^{N_L} \omega_j f_j - \omega_i f_i}, \quad k = 1, \ldots, N_L, k \neq i. \tag{35}$$

Then we assign $F_k \to f_k, k = 1, \ldots, N_L$ and go to the next i. The above procedure will stop after at most N_L steps.

Eq. (35) indicates that all the other elements f_k are scaled down by a positive factor $\alpha = M_0 / \left(\sum_{j=1}^{N_L} \omega_j f_j - \omega_i f_i\right) \leq 1$ and F_k has the same positivity/negativity as f_k. The new $F_1, \ldots, F_{N_L}$ can keep the zeroth-order moment M_0 since

$$\sum_{k=1}^{N_L} \omega_k F_k = \omega_i F_i + \sum_{k=1, k\neq i}^{N_L} \left(\omega_k f_k \cdot \frac{M_0}{\sum_{j=1}^{N_L} \omega_j f_j - \omega_i f_i} \right) = M_0 \frac{\sum_{k\neq i}^{N_L} \omega_k f_k}{\sum_{j\neq i}^{N_L} \omega_j f_j} = M_0.$$

4. Numerical results

In this section we present three numerical examples with different forms of source terms in Eq. (1). The QBMMs solve the moment transport equations (21) using the fifth-order WENO-MZ finite difference scheme [52] for the convection term, the second-order central scheme for the diffusion term, and the third-order TVD-Runge Kutta method [53,54] for the time marching in which the mixing and source integral terms are treated explicitly. The source integral term in Eq. (21) is calculated using Eq. (30) in the QMOM or Eq. (33) in the LQMOM. The time step $\Delta t = 10^{-4}$, and the grid size $\Delta x = 10^{-3}$. The quadrature nodes $N_q = 2$ is adopted for the QMOM, and the LQMOM predefines $N_L = 8$ Gauss points in the interval $v \in [0.8, 1.2]$ as per experience. The above values of Δt and Δx are also used for the mesh-based Monte Carlo method with the sampling number per mesh cell $N_E = 20$. To obtain a reference solution we also carry out DNS for the Burgers equation with $\Delta t = 10^{-4}$ and $\Delta x = 2.5 \times 10^{-4}$ by employing the same spatial and temporal discretization schemes. In all the examples, the computational domain is $[-1, 1]$ with periodic boundary conditions on both ends. For consistency, the initial conditions given should have the periodicity.

4.1. Decaying Burgers turbulence with random initial conditions

First, we consider the decaying Burgers turbulence with a random initial condition. The source term in Eq. (1) is:

$$S(u, x, t) = 0. \tag{36}$$

The initial condition is composed of n sin waves superimposed on unit velocity:

$$u(x, 0) = \sum_{i=1}^{N} \left(2E_0(k_i)\right)^{\frac{1}{2}} \sin(k_i \pi x + \beta_i) + 1, \tag{37}$$

which is periodic at the two boundaries. The initial energy spectrum $E_0(k)$ is given in the Fourier space mimicking the turbulence spectrum. In this work, the following initial spectrum is used as in [14],

$$E_0(k) = \begin{cases} A5^{-\frac{5}{3}}, & 1 \le k \le 5, \\ Ak^{-\frac{5}{3}}, & k > 5. \end{cases} \tag{38}$$

Here, the reduced wavenumber k_i is taken to be an integer varying from 1 to 1280 and $N = 1280$. For each k_i, the velocity u has a uniformly random phase angle $\beta_i \in [-\pi, \pi]$. The constant A is determined to make the turbulence intensity $u'/\bar{u} = 0.7\%$, where $u' = \sqrt{\sum_{i=1}^{N}(u_i - \bar{u})^2/N}, \bar{u} = 1$.

For $t > 0$, the instantaneous turbulent kinetic energy spectrum is computed as follows:

$$E(\kappa, t) = \frac{L}{2\pi} C |\hat{u}(\kappa, t)|^2 = \frac{L}{2\pi} C \left| \frac{1}{L} \int_{-L/2}^{L/2} u'(x, t) e^{-i\kappa x} \mathrm{d}x \right|^2, \kappa = \frac{2\pi j}{L}, j = 0, \ldots, \frac{N_x}{2}, C = \begin{cases} \frac{1}{2} & \text{if } j = 0 \\ 1 & \text{otherwise} \end{cases}, \tag{39}$$

where L is the length of the computational domain, N_x is the total number of grid cells, $\hat{u}(\kappa, t)$ is the Fourier transformation of the fluctuating velocity $u'(x, t) = u(x, t) - \langle u \rangle(t)$, and the operator $\langle \cdot \rangle$ denotes the space average.

The computation is processed to the end time $t_{\text{end}} = 0.05$ when the solution is still smooth [14]. Fig. 1 shows the turbulent kinetic energy spectrums computed with DNS, MC, QMOM and LQMOM. Hereafter k is a reduced wavenumber defined as $k = \kappa L/2\pi$ as in [19] where κ is the original wavenumber in Eq. (39) and $L = 2$ is the length of the domain. It is seen that all the results deviate from $E_0(k)$ at high wavenumbers but agree very well with it at low wavenumbers. The MC result shows remarkably smaller dissipation at high wavenumbers. This is probably due to the fact that the Monte Carlo method is essentially a Lagrangian method with low dissipation, and the stochastic Wiener process in each update of the particle velocity may help maintain the turbulent intensity. The results by QMOM and LQMOM are close to each other and agree well with the DNS result for the wavenumber range $\log_{10} k < 2$.

4.2. White-in-time random force-driven Burgers equation

Second, we consider the randomly forced Burgers equation problem as studied in [19,55–57]. The source term in Eq. (1) is an additive forcing term which takes the specific form [19,58],

$$S(u, x, t) = S(x, t) = \frac{A}{\sqrt{\Delta t}} \sum_{n=1}^{N_c} \frac{Z_n(t)}{\sqrt{\pi n}} \cos\left(\frac{2\pi n}{L} x\right), \tag{40}$$

where A is the amplitude of the fluctuations, for which we have adopted the value $A = 0.04$ as used by Manzanero [59]. This source term results from the sum of N_c harmonic modes, whose amplitude, $Z_n(t)/\sqrt{\pi n}$, includes a standard normal distribution $Z_n(t)$. $L = 2$ is the length of the computational domain. The number of modes $N_c = 80$.

The initial condition is $u(x, 0) = 1$ which satisfies the periodicity. The end time is $t_{\text{end}} = 600$. Due to the low amplitude of the source term, $A = 0.04$, the solution remains positive, and its average is close to $u = 1$.

We compare the energy spectrums in Fig. 2. The energy spectrum is computed using Eq. (39) and time-averaged from $t = 200$ to $t = 600$ as done in [58]. It is seen that the present LQMOM result is in good agreement with the DNS for wavenumbers in the range

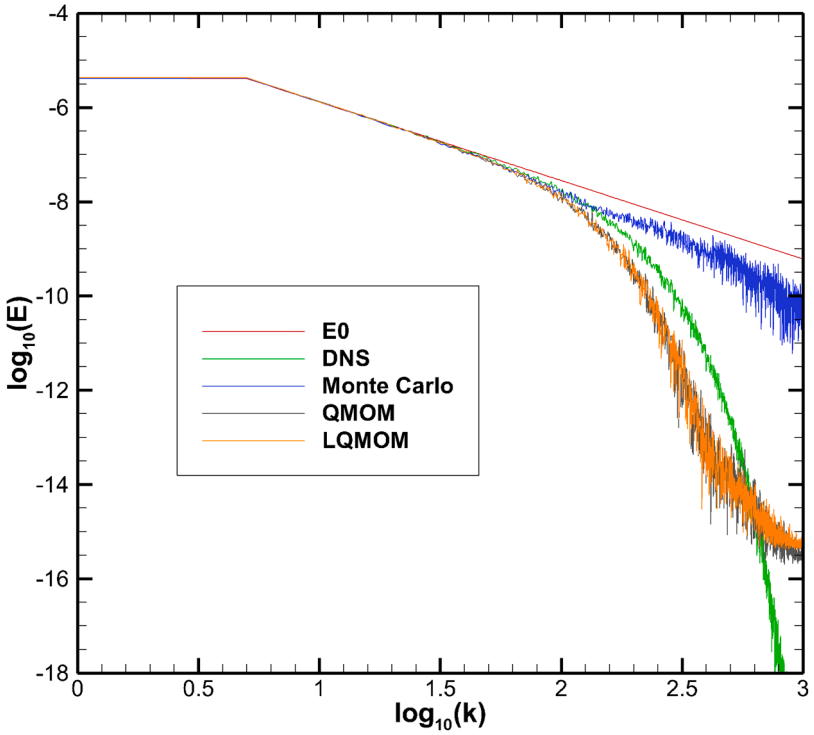

Fig. 1. Comparison of turbulent energy spectrums at time $t_{end} = 0.05$ among DNS, Monte Carlo, QMOM and LQMOM for decaying Burgers turbulence with the zero source (36) and the random initial condition (37).

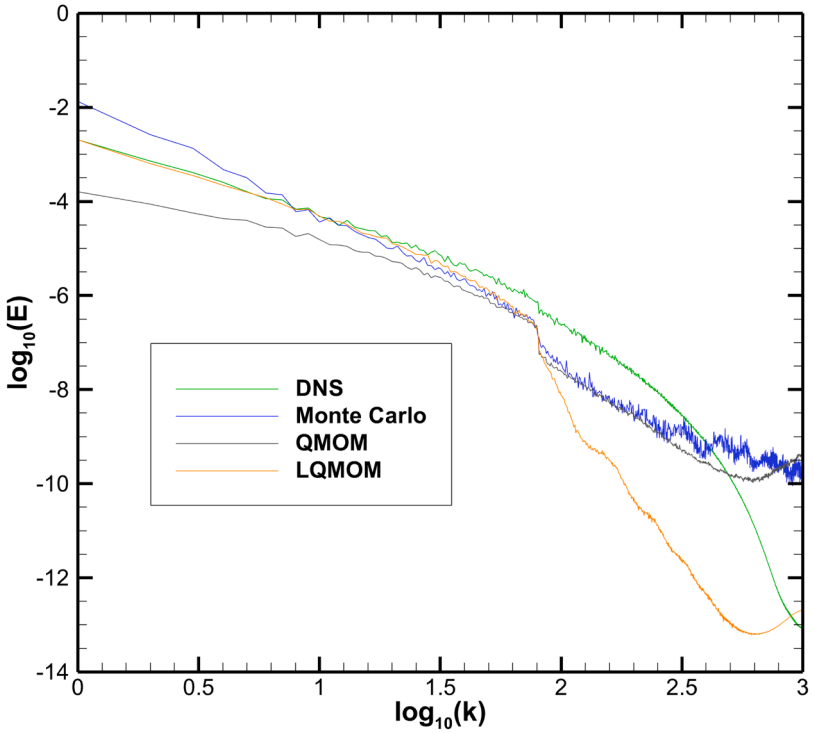

Fig. 2. Comparison of time-averaged turbulent energy spectrum among the DNS, Monte Carlo, QMOM and LQMOM for the forced Burgers turbulence problem with the source (40).

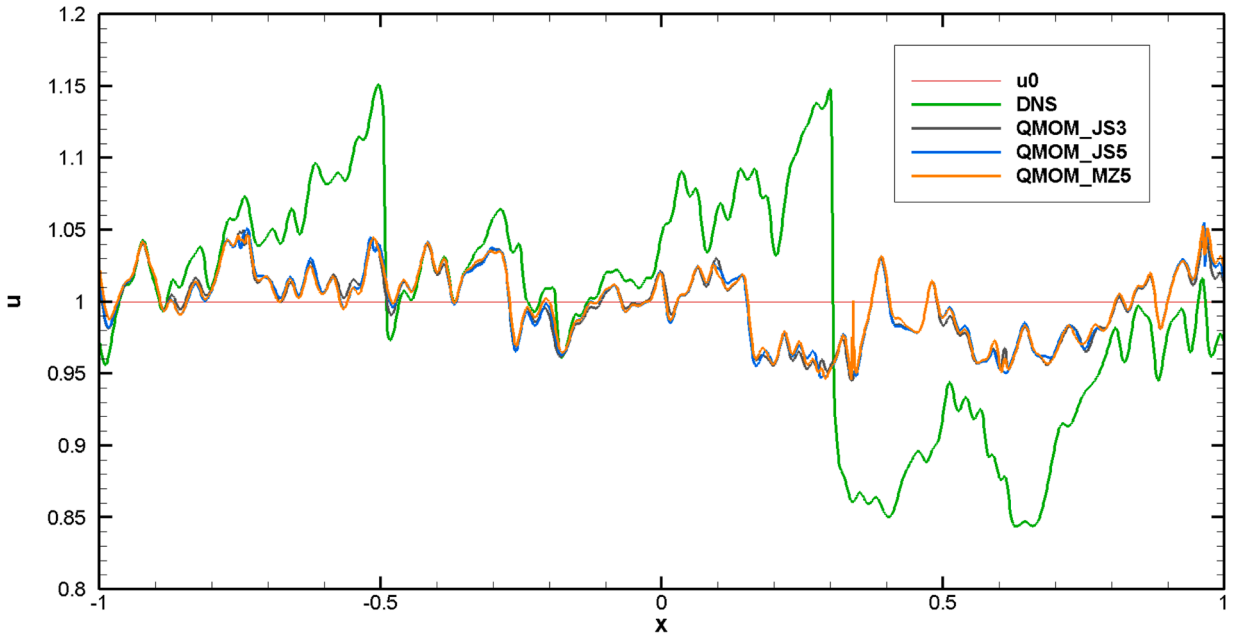

(a)

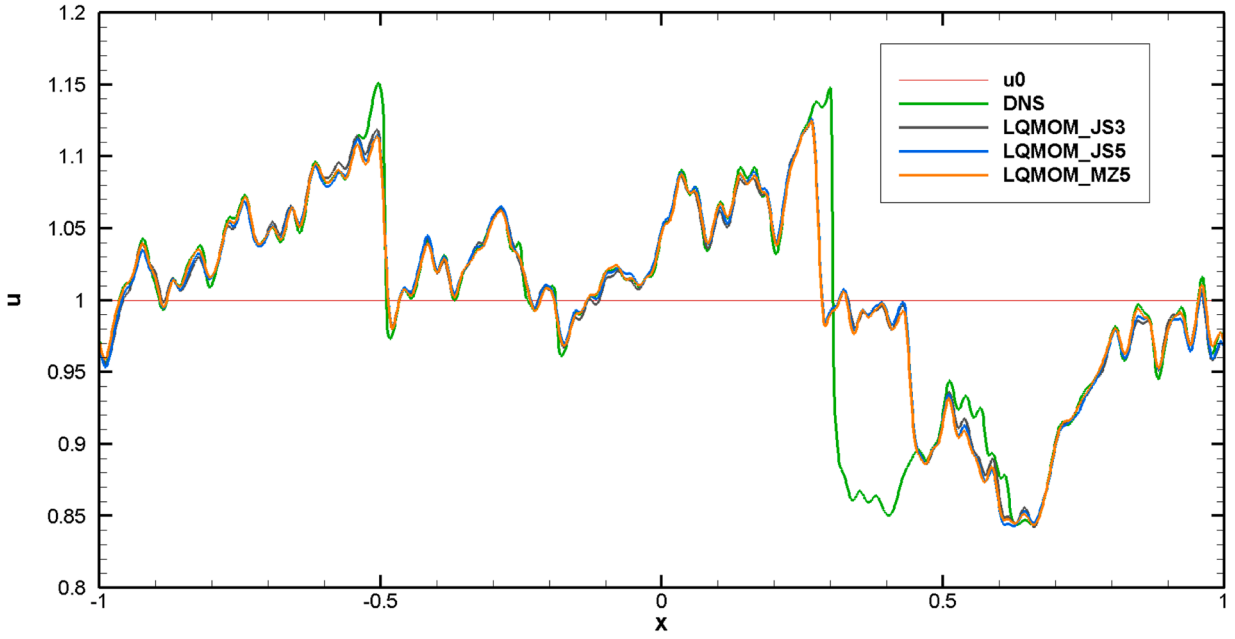

(b)

Fig. 3. Comparison of the solution snapshots between the DNS and the two QBMMs (QMOM (a), LQMOM (b)) for forced Burgers turbulence problem with the source (40) at time $t_{\text{end}} = 600$. "JS3/JS5" means third-order/fifth-order WENO-JS scheme [60].

$\log_{10} k < 1.5$ but it is more dissipative at high wavenumbers. The QMOM has rather lower values at low frequencies than the LQMOM. The reason is that it only uses two quadrature nodes ($N_q = 2$) and thus the approximation accuracy is not good. The MC result predicts higher values at low wavenumbers. The reason may be that the frequent operations of adding and/or deleting particles are carried out independently within a sample volume in the present implementation, which may inappropriately introduce turbulent motion at low wavenumbers. Notice that there is an evident drop at $\log_{10} k = \log_{10} N_c \approx 1.90$ for all the simulation results. This drop marks the dividing line between the low wavenumber range ($k < N_c$) in which the turbulent motion is directly affected by the forcing term

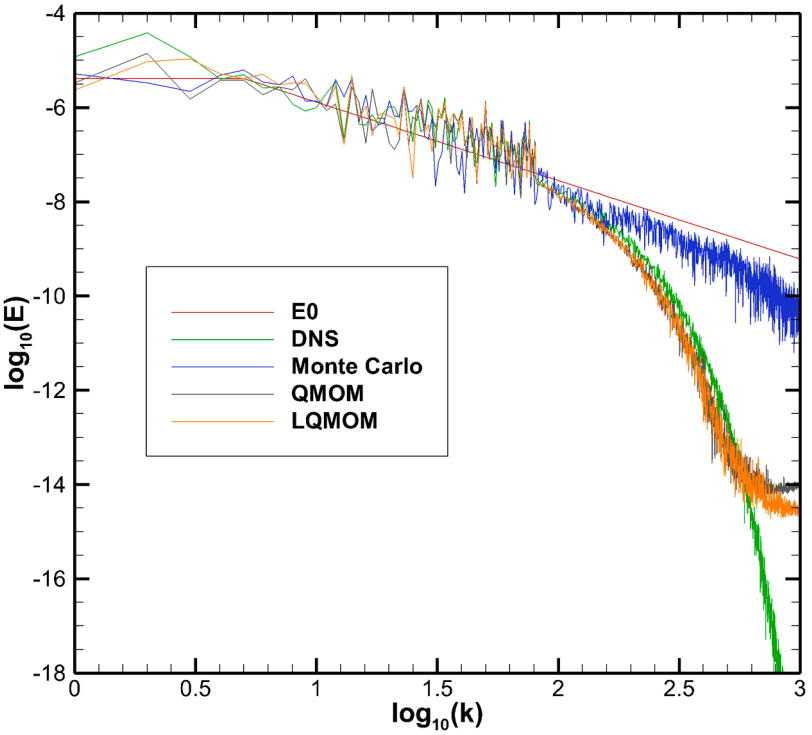

Fig. 4. Comparison of turbulent energy spectrums among DNS, Monte Carlo, QMOM and LQMOM for the Burgers equation with the nonlinear source (41) at the time $t_{\text{end}} = 0.05$.

(40) and the high wavenumber range ($k > N_c$) in which the turbulent motion is mainly controlled by the intrinsic mechanism of the discretized Burgers equation.

Fig. 3 compares the final-time solution profiles between the two QBMMs with various WENO schemes [52,60] and the DNS with the WENO scheme [52]. From Fig. 3a we can observe that the QMOM results with three different WENO schemes are similar, however, they deviate much from the DNS result. The velocity profile computed by the MC method fluctuates similarly but has very different phases so we do not plot it. Fig. 3b shows that the LQMOM results with three different WENO schemes match fairly well with the DNS result. However, larger discrepancies occur at $x \approx -0.5$ and $x \approx 0.3$, which may be attributed to shock waves formed at these positions.

4.3. Nonlinear random force-driven Burgers equation

Third, we consider a nonlinear random forcing term, which explicitly depends on the solution u and is also white-in-time,

$$S(u,x,t) = \frac{Au(2-u)}{\sqrt{\Delta t}} \sum_{n=1}^{N_c} \frac{Z_n(t)}{\sqrt{\pi n}} \cos\left(\frac{2\pi n}{L} x\right), \tag{41}$$

where $A = 0.04$ and $Z_n(t)$ is a standard normal distribution in order to bring randomness process in time to the Burgers equation (1). The initial condition is the same as Eq. (37) with Eq. (38). The simulation end time $t_{\text{end}} = 0.05$.

The energy spectrums at $t_{\text{end}} = 0.05$ computed with different methods are compared in Fig. 4. It is seen that the results computed by QMOM and LQMOM match with the DNS result up to the wavenumber $\log_{10} k \approx 2.7$, but the MC result matches with the DNS result only for the range $\log_{10} k < 2.2$. It is noted that all the computed results in the range $\log_{10} k < \log_{10} N_c \approx 1.9$ have larger fluctuations as the external forcing is only available for $n < N_c$ in (41).

Finally, Table 1 shows CPU times taken by various methods for running this example to $t_{\text{end}} = 0.05$, in which the DNS uses a fine grid of $\Delta x = 2.5 \times 10^{-4}$ and the MC and QBMM use a coarse grid of $\Delta x = 10^{-3}$, and the time steps roughly correspond to a CFL number of 0.25. We see that the LQMOM takes less CPU time than the QMOM and DNS. The DNS method solves only one transport equation on a four times finer grid, while the LQMOM with $N_L = 8$ quadrature nodes solves 8 equations, and the QMOM with $N_q = 2$ solves 4 equations on a coarse grid. All the compared methods are implemented with OpenMP on a single node. However, the MC method, which is not well parallelized, runs slower than the others.

Table 1
CPU times in seconds by different methods for computing the Burgers equation (1) with the nonlinear source term (41) from $t = 0$ to $t = 0.05$. Grid cells $N_{\mathrm{DNS}} = 8000$, $N_{\mathrm{QBMM}} = N_{\mathrm{MC}} = 2000$, time step sizes $\Delta t_{\mathrm{DNS}} = 10^{-4}$, $\Delta t_{\mathrm{QBMM}} = \Delta t_{\mathrm{MC}} = 4 \times 10^{-4}$.

LQMOM	QMOM	DNS	Monte Carlo
15.460	18.984	27.920	31.523

5. Conclusion

We have developed a transported PDF model and one of its numerical methods for simulating one-dimensional Burgers turbulence driven by random forces and random initial data. An exact one-point one-time velocity PDF transport equation for the one-dimensional Burgers equation with a nonlinear stochastic source term is derived first, and then the conditional advection and conditional diffusion terms are closed by using two respective models. The lumped gradient model is proposed to close the conditional advection term, enabling the corresponding moment transport equations to be strictly hyperbolic. Numerical solutions of the modeled PDF equation are carried out by employing the Lagrangian Monte Carlo particle method, the original quadrature method of moments and the linear quadrature method of moments with positivity-preserving modification. Comparisons between the numerical results with the above three methods and with the DNS for the considered Burgers turbulence problems demonstrated that 1) the present transported PDF model is viable for studying statistic properties of the Burgers equation with a stochastic driving force, and 2) the modified LQMOM is more efficient than the QMOM and Monte Carlo particle method employed.

There are some limitations of the transported PDF approach. The conditional advection and diffusion terms still require phenomenological closure models (e.g., lumped-gradient and IEM-type models), whose generality remains to be assessed. In addition, the one-point PDF framework cannot directly capture multi-point spatial correlations, and thus spectral/intermittency/shock-clustering information is only indirectly captured via modeling and numerical resolution. Finally, the method involves model parameters (e.g., C_Ω and C_S) that may need calibration, and extensions to higher dimensions and joint PDFs demand sophisticated numerics. Dealing with these limitations are our future work.

CRediT authorship contribution statement

Yize Wang: Methodology, Software, Data curation, Visualization, Writing – original draft, Writing – review & editing; **Li Yuan:** Conceptualization, Methodology, Writing – review & editing, Funding acquisition, Supervision.

Data availability

Data will be made available on request.

Declaration of competing interest

The authors declare that they have no known competing financial interests or personal relationships that could have appeared to influence the work reported in this paper

Acknowledgements

The authors thank Y. C. Wang and K. C. Zhao for their help in the initialization of this work. The computations are carried out on the high performance computer of the State Key Laboratory of Mathematical Sciences and the supercomputer of Computer Network Information Center, Chinese Academy of Sciences, and Beijing Super Cloud Computing Center.

References

[1] J.M. Burgers, A mathematical model illustrating the theory of turbulence, Adv. Appl. Mech. 1 (1948) 171–199. https://doi.org/10.1016/S0065-2156(08)70100-5
[2] J.M. Burgers, On the emergence of patterns of order, Bull. Am. Math. Soc. 69 (1) (1963) 1–25.
[3] S. Kida, Asymptotic properties of Burgers turbulence, J. Fluid Mech. 93 (1979) 337–377. https://doi.org/10.1017/S0022112079001932
[4] T. Gotoh, R.H. Kraichnan, Statistics of decaying Burgers turbulence, Phys. Fluids A: Fluid Dyn. 5 (2) (1993) 445–457. https://doi.org/10.1063/1.858868
[5] M. Avellaneda, E. Weinan, Statistical properties of shocks in Burgers turbulence, Commun. Math. Phys. 172 (2) (1995) 13–38. https://doi.org/10.1007/BF02104509
[6] S.N. Gurbatov, S.I. Simdyankin, E. Aurell, U. Frisch, G. Toth, On the decay of Burgers turbulence, J. Fluid Mech. 344 (1997) 339–374. https://doi.org/10.1017/S0022112097006241
[7] A. Bahraminasab, M.D. Niry, J. Davoudi, M. Reza Rahimi Tabar, A.A. Masoudi, K.R. Sreenivasan, Taylor's frozen-flow hypothesis in Burgers turbulence, Phys. Rev. E 77 (2008) 065302. https://doi.org/10.1103/PhysRevE.77.065302
[8] G. Menon, R. Srinivasan, Kinetic theory and Lax equations for shock clustering and Burgers turbulence, J. Stat. Phys. 140 (2010) 1195–1223. https://doi.org/10.1007/s10955-010-0028-3

[9] M.D. Love, Subgrid modelling studies with Burgers' equation, J. Fluid Mech. 100 (1) (1980) 87–110. https://doi.org/10.1017/S0022112080001024
[10] Y.M. Dakhoul, K.W. Bedford, Improved averaging method for turbulent flow simulation. Part I: Theoretical development and application to Burgers' transport equation, Int. J. Numer. Methods Fluids 6 (2) (1986) 49–64. https://doi.org/10.1002/fld.1650060202
[11] A. Das, R.D. Moser, Optimal large-eddy simulation of forced Burgers equation, Phys. Fluids 14 (2002) 4344–4351.
[12] S. Basu, Can the dynamic eddy-viscosity class of subgrid-scale models capture inertial-range properties of Burgers turbulence?, J. Turbul. 10 (12) (2009) 1–16.
[13] H. Cho, D. Venturi, G.E. Karniadakis, Statistical analysis and simulation of random shocks in stochastic Burgers equation, Proc. R. Soc. A 470 (2014) 20140080. http://dx.doi.org/10.1098/rspa.2014.0080
[14] Y.N. Li, Z.J. Wang, A priori and a posteriori evaluations of sub-grid scale models for the Burgers' equation, Comput. Fluids 139 (2016) 92–104.
[15] R. Maulik, O. San, Explicit and implicit LES closures for Burgers turbulence, J. Comput. Appl. Math. 327 (2018) 12–40.
[16] E. Amani, A. Ahmadpour, M.J. Aghajari, Dynamic subgrid-scale LES model for turbulent non-Newtonian flows: A priori and a posteriori analyses of Burgers turbulence, J. Nonnewton Fluid Mech. 295 (2021) 104615. https://doi.org/10.1016/j.jnnfm.2021.104615
[17] C.A.J. Fletcher, Computational Techniques for Fluid Dynamics 1: Fundamental and General Techniques, Springer-Verlag, Berlin, Heidelberg, GmbH, Berlin, Heidelberg, GmbH, 1991.
[18] P. Düben, D. Homeier, K. Jansen, D. Mesterhazy, G. Münster, C. Urbach, Monte Carlo simulations of the randomly forced Burgers equation, EPL 84 (2008) 40002. https://doi.org/10.1209/0295-5075/84/40002
[19] P. Solán-Fustero, A. Navas-Montilla, E. Ferrer, J. Manzanero, P. García-Navarro, Application of approximate dispersion-diffusion analyses to under-resolved Burgers turbulence using high resolution WENO and UWC schemes, J. Comput. Phys. 435 (2021) 110246. https://doi.org/10.1016/j.jcp.2021.110246
[20] T. Gotoh, Probability density functions in steady-state Burgers turbulence, Phys. Fluids 11 (1999) 2143–2148. https://doi.org/10.1063/1.870106
[21] W. Kollmann, The PDF approach to turbulent flow, Theoret. Comput. Fluid Dyn. 1 (1990) 249–285.
[22] C. Dopazo, Recent developments in PDF methods, in: P.A. Libby, F.A. Williams (Eds.), Turbulent Reacting Flows, Chapter 7, Academic Press, London, 1994, pp. 375–474.
[23] S. Heinz, Statistical Mechanics of Turbulent Flows, Springer-Verlag, New York, New York, 2003.
[24] S.B. Pope, A Monte Carlo method for the PDF equations of turbulent reactive flow, Combust. Sci. Technol. 25 (1981) 159–174.
[25] L. Valiño, A field Monte Carlo formulation for calculating the probability density function of a single scalar in a turbulent flow, Flow Turbul. Combust. 60 (1998) 157–172.
[26] F.A. Jaberi, P.J. Colucci, S. James, P. Givi, S.B. Pope, Filtered mass density function for large-eddy simulation of turbulent reacting flows, J. Fluid Mech. 401 (1999) 85–121.
[27] P. Givi, Filtered density function for subgrid scale modeling of turbulent combustion, AIAA J. 44 (1) (2006) 16–23.
[28] J.M. Hammersley, D.C. Handscomb, Monte Carlo Methods, Methuen Press, London, London, 1964.
[29] S.B. Pope, PDF methods for turbulent reactive flows, Prog. Energy Combust. Sci. 11 (2) (1985) 119–192.
[30] S.B. Pope, Lagrangian PDF methods for turbulent flows, Annu. Rev. Fluid Mech. 26 (1994) 23–63.
[31] F. Wang, R. Liu, L. Dou, D.H. Liu, J. Jin, A dual timescale model for micro-mixing and its application in LES-TPDF simulations of turbulent nonpremixed flames, Chin. J. Aeronaut. 32 (4) (2019) 875–887.
[32] S.J. Xu, S.H. Zhong, F. Zhang, X.S. Bai, On element mass conservation in Eulerian stochastic fields modeling of turbulent combustion, Combust. Flame 239 (2022) 111577.
[33] R. McGraw, Description of aerosol dynamics by the quadrature method of moments, Aerosol Sci. Technol. 27 (1997) 255–265.
[34] D.L. Marchisio, J.T. Pikturna, R.O. Fox, R.D. Vigil, A.A. Barresi, Quadrature method of moments for population-balance equations, AlChE J. 49 (2003) 1266–1276.
[35] C. Yuan, F. Laurent, R.O. Fox, An extended quadrature method of moments for population balance equations, J. Aerosol Sci. 51 (2012) 1–23.
[36] C. Yuan, R.O. Fox, Conditional quadrature method of moments for kinetic equations, J. Comput. Phys. 230 (22) (2011) 8216–8246.
[37] P.C.R. Taunay, M.E. Mueller, Quadrature-based moment methods for kinetic plasma simulations, J. Comput. Phys. 473 (2023) 111700.
[38] V. Raman, H. Pitsch, R.O. Fox, Eulerian transported probability density function sub-filter model for large-eddy simulations of turbulent combustion, Combust. Theor. Model. 10 (2006) 439–458.
[39] P. Donde, H. Koo, V. Raman, A multivariate quadrature based moment method for LES based modeling of supersonic combustion, J. Comput. Phys. 231 (2012) 5805–5821.
[40] S. Salenbauch, A. Cuoci, A. Frassoldati, C. Saggese, T. Faravelli, C. Hasse, Modeling soot formation in premixed ames using an extended conditional quadrature method of moments, Combust. Flame 162 (2015) 2529–2543.
[41] E. Madadi-Kandjani, Quadrature-based models for multiphase and turbulent reacting flows, Ph.D. thesis, Iowa State University, 2017.
[42] C. Dopazo, E.E. O'Brien, An approach to the autoignition of a turbulent mixture, Acta Astronaut. 1 (1974) 1239–1266.
[43] J. Villermaux, L. Falk, A generalized mixing model for initial contacting of reactive fluids, Chem. Eng. Sci. 49 (1994) 5127–5140.
[44] S.B. Pope, Turbulent Flows, Cambridge University Press, 2000.
[45] Y.C. Wang, Y.Z. Wang, L. Yuan, Linear quadrature method of moments for solving the transported probability density function model for turbulent combustion, Combust. Theor. Model. 29 (2) (2025) 145–176. https://doi.org/10.1080/13647830.2025.2463893
[46] R. McDermott, S.B. Pope, A particle formulation for treating differential diffusion in filtered density function methods, J Comput Phys 226 (2007) 947–993.
[47] R.O. Fox, Computational Models for Turbulent Reacting Flows, Cambridge University Press, Cambridge, Cambridge, 2003.
[48] R. Mokhtarpoor, H. Turkeri, M. Muradoglu, A new robust consistent hybrid finite-volume/particle method for solving the PDF model equations of turbulent reactive flows, Comput. Fluids 105 (10) (2014) 39–57.
[49] R.G. Gordon, Error bounds in equilibrium statistical mechanics, J. Math. Phys. 9 (5) (1968) 655–663.
[50] R.A. Sack, A.F. Donovan, An algorithm for Gaussian quadrature given modified moments, Numer. Math. 18 (1971/72) 465–478.
[51] J.C. Wheeler, Modified moments and Gaussian quadrature, Rocky Mountain J. Math. 4 (1974) 287–296.
[52] Y.Z. Wang, K.L. Zhao, L. Yuan, A modified fifth-order WENO-Z scheme based on the weights of the reformulated adaptive order WENO scheme, Int. J. Numer. Methods Fluids 96 (10) (2024) 1631–1652.
[53] S. Gottlieb, C.W. Shu, Total variation diminishing Runge-Kutta schemes, Math. Comput. 67 (221) (1998) 73–85.
[54] S. Gottlieb, C.-W. Shu, E. Tadmor, Strong stability-preserving high-order time discretization methods, SIAM Rev. 43 (1) (2001) 89–112.
[55] J. Bec, K. Khanin, Burgers turbulence, Phys. Rep. 447 (1) (2007) 1–66. https://doi.org/10.1016/j.physrep.2007.04.002
[56] A. Chekhlov, V. Yakhot, Kolmogorov turbulence in a random-force-driven Burgers equation, Phys. Rev. E 51 (1995) R2739–R2742. https://doi.org/10.1103/PhysRevE.51.R2739
[57] O. Zikanov, A. Thess, R. Grauer, Statistics of turbulence in a generalized random-force-driven Burgers equation, Phys. Fluids 9 (5) (1997) 1362–1367. https://doi.org/10.1063/1.869250
[58] R.C. Moura, S.J. Sherwin, J. Peiró, Linear dispersion-diffusion analysis and its application to under-resolved turbulence simulations using discontinuous Galerkin spectral/hp methods, J. Comput. Phys. 298 (2015) 695–710.
[59] J. Manzanero, Dispersion-diffusion analysis for variable coefficient advection problems, with application to alternative DG formulations and under-resolved turbulence, Master's thesis, Universidad Politécnica de Madrid, 2016. https://oa.upm.es/63199
[60] G.S. Jiang, C.W. Shu, Efficient implementation of weighted ENO schemes, J. Comput. Phys. 126 (1) (1996) 202–228. https://doi.org/10.1006/jcph.1996.0130